ACTIVE JOINT FAILURE ANALYSIS OF PARALLEL MANIPULATORS

Mahir Hassan
Department of Mechanical Engineering
Queen's University
Kingston, Ontario, Canada K7L 3N6
e-mail: mhassan@me.queensu.ca

Leila Notash
Department of Mechanical Engineering
Queen's University
Kingston, Ontario, Canada K7L 3N6
e-mail: notash@me.queensu.ca

Abstract

In this study, the effect of active joint jam and actuator force loss on the mobility, velocity and static force of parallel manipulators is investigated. The Grübler's mobility equation is modified to take into account the motion space of the manipulator branches. To predict the post-failure performance of parallel manipulators, the effect of joint jam and actuator force loss on the velocity and on the force of parallel manipulators is investigated by examining the change in the Jacobian matrix, its inverse and transposes. The methodology is implemented in a simulation of a 3-3 6-degree-of-freedom (6-DOF) Stewart-Gough manipulator in various configurations, and reduced velocity and force performance is investigated.

1. Introduction

1.1 Parallel Manipulators

Robots are programmable machines that can be programmed according to their task requirements. Parallel robots, unlike serial robots, have closed-chain mechanisms, in which a number of serial branches (also called limbs or legs) act in parallel on a mobile platform, as shown in Figure 1. Generally speaking, parallel manipulators have higher stiffness and motion accuracy than serial manipulators due to the in-parallel application of the branches on the mobile platform.

1.2 Failure of Parallel Robots

Robot failure is the inability of the robot to perform its required function. Failure of parallel robots could originate from various components such as links, passive joints, active joints and end-effector. In active joints, there are several components that are susceptible to failure, such as actuator devices, transmission systems, sensors and controllers. Potential failure modes of active joints, are joint jam, actuator run-away, degradation in actuator force and complete loss of actuator force. All the above failure modes may render the parallel manipulator incapable of completing its tasks.

A fault tolerant robot is capable of completing its task with the presence of failure. Fault tolerance could be achieved by compensating the function of the failed hardware component by the function of a redundant component that is initially incorporated in the design. Robot manipulators with redundant components are called redundant manipulators.

Figure 1: A 6-DOF parallel robot (F-200i) from FANUC Robotics Inc.

1.3 Previous Works

Failure and its effect on the performance of serial robots have been studied by many researchers; a list of some relevant work is included in Visinsky et al. (1994). Roberts and Maciejewski (1996) studied the effect of locked joint failure on manipulability index of redundant serial manipulators. The change in the manipulability value due to locked joint failure at a certain configuration, was used as a local fault tolerance measure that indicated how close the serial manipulator came to singularity when one or more of its joints were locked in a specific configuration.

Bergerman and Xu (1997) studied the effect of locking a free-swinging joint, whose torque generation capability was completely lost, on the workspace and manipulability of a planar redundant serial manipulator. English and Maciejewski (1998) studied free-swinging joint failure in serial manipulators and defined three measures (torque, acceleration and swing-angle) that quantitatively reflect the susceptibility of the serial manipulators to the occurrence of free-swinging failure and to its potential post-failure damage. It was suggested that minimizing these measures would minimize the likelihood of the occurrence of free-swinging failure and its post-failure consequences. Roberts (2001) studied the effect of locking and unlocking of single and multiple free-swinging failed joints on static and dynamic manipulability of redundant serial robots.

For parallel manipulators, however, research on failure analysis and fault tolerance has not been sufficiently explored. Notash and Huang (2003) used the Failure Mode and Effect Analysis to study the failure modes of parallel manipulators with their effects on the degree of freedom (DOF), actuation and constraint in parallel manipulators. Redundancy types, such as redundant DOF, redundant actuation, redundant branch and redundant sensing, were suggested for fault

tolerant design. Several actuation redundancy configurations of parallel robots with various degrees of mobility were listed, showing the distribution of redundant actuators on the branches. The effects of various failure modes and the required redundancy to cope with these failure modes were suggested.

Ting et al. (1995) presented two fault tolerance methods for post-failure recovery against full or partial loss of actuator torque in parallel robots. The first method was based on utilizing actuation redundancy in which the amount of lost torque was compensated by the redundant actuators. In this case, the torque was re-distributed on other actuators. The second method was based on changing the task time, which effectively changed the inertial forces, to decrease the overall actuator torque demands.

1.4 Contribution and Organization of this Work

This study is aimed at analyzing the effect of active joint failure on mobility, velocity and force of parallel manipulators. An analytical procedure to determine the mobility, velocity and force capability of parallel manipulators after failure is explored. The procedure could be useful to predict, in cases where maintenance is not immediately available, whether or not the manipulator could perform the task or part of the task successfully with the existence of failure.

A modified mobility equation is presented which addresses the effect of the type of joints on mobility of parallel manipulators, followed by an illustration of the effect of active joint jam and actuator force loss on mobility. A brief background on velocity and static force analyses in parallel manipulators is given. The effect of active joint failures, such as joint jam and actuator force loss on velocity and static force is analyzed. The analysis procedure is applied on an example spatial parallel manipulator.

2. Analysis of Active Joint Failure in Parallel Manipulators

In this section, the effect of active joints failure on the mobility, velocity and force of the manipulator is investigated. Two catastrophic failures are considered: joint jam and actuator force loss.

Joint jam is the case when a joint loses its DOF and, as a result, its velocity becomes zero. This failure could occur due to bearing jam, actuator brake failure to release, actuator breakdown in a non back-drivable joint, and so on. Also, the joint may be locked by the operator.

Actuator force loss is the case when the actuator loses its entire force generation capability and as a result, the joint becomes a passive joint if the joint driving system is back−drivable. However, if the joint driving system is not back−drivable, it jams. A parallel manipulator could also lose actuator force if the branch of that actuator is broken off the manipulator, in which case the manipulator loses an active branch.

2.1 Effect of Active Joint Failure on Manipulator Mobility

2.1.1 Modifying Grübler's Mobility Equation

The mobility of parallel manipulators could generally be calculated from Grübler's equation, written as:

$$M = \lambda(l - n - 1) + \sum_{j=1}^{n} f_j \tag{1}$$

where M is the mobility (DOF) of the manipulator; l is the total number of links in the manipulator, including the fixed (base) link; n is the total number of all single and multiple-DOF joints in the manipulator; f_j is the DOF of the jth joint; λ is the DOF of the space in which the manipulator is intended to function and is equal to 3 for planar or spherical manipulators and 6 for spatial manipulators.

Although equation (1) is sufficient for a preliminary analysis, it provides only the minimum possible mobility for a particular manipulator, Malik and Kerr (1992), as the equation does not take into account the geometrical relations between the joints. Also, equation (1) does not give the correct mobility for manipulators where the motion space DOF, λ, varies due to constraints imposed by the kinematic structure or geometry, Liu and Yu (1995) and Zhang (2000). For example, the mobility of the planar manipulator in Figure 2 is 1, if λ=3 is used in equation (1). However, because λ is not the same for all the links, the actual observed mobility is 2. The joints of the branch containing links 2 and 3 are revolute joints that provide motion in three directions, i.e., two translations in the plane of the manipulator and one rotation about an axis normal to the plane. Therefore, the DOF of the motion space for the branch containing links 2 and 3 is 3. On the other hand, the joints of the two branches containing links 5 and 6 are prismatic joints that provide motion in two translations on the plane, and, therefore, the DOF of the motion space of each one of these two branches is 2.

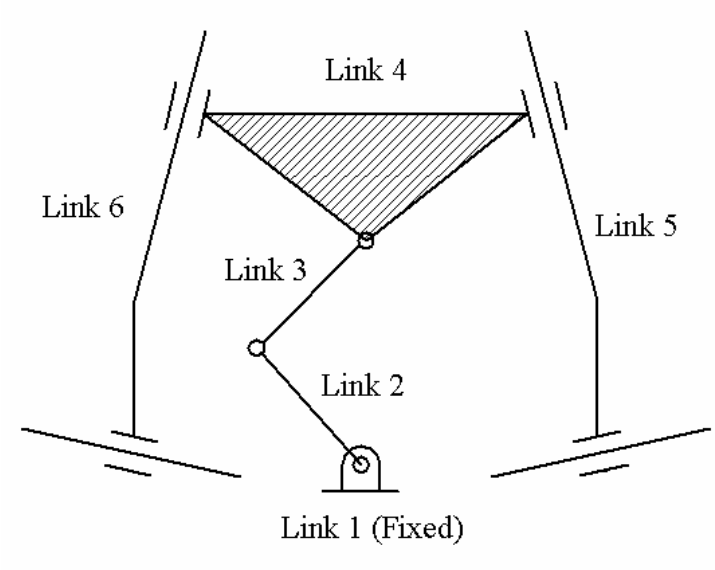

Figure 2: A six-link 2-DOF planar manipulator

To calculate the mobility for manipulators like the one in Figure 2 and to understand the effect of losing branches from, or adding branches to the parallel manipulator, equation (1) has been modified as shown in the following procedure.

The mobility of manipulators could be written as:

$$M = \sum_{i=1}^{L} (\lambda_i \, l_i) + \lambda_p - \sum_{i=1}^{L} \sum_{j=1}^{n_i} (\lambda_i - f_{ij}) \;\; : \;\; \lambda_p = \min(\lambda_1, ..., \lambda_i, .., \lambda_L) \qquad (2)$$

where L is the number of branches (or limbs) of the manipulator; l_i is the number of links in the ith branch, not including the base link and the mobile platform; λ_i is the DOF of the motion space provided by the joints of the ith branch; λ_p is the DOF of the motion space of mobile platform; n_i is the number of joints in the ith branch; and f_{ij} is the DOF of the jth joint in the ith branch.

The term $\sum_{i=1}^{L} (\lambda_i \, l_i) + \lambda_p$ is the sum of the DOF of the spaces of all links. It should be noted that the DOF of the space for the fixed base link is 0, and therefore, was not included in equation (2).

The term $\sum_{i=1}^{L} \sum_{j=1}^{n_i} (\lambda_i - f_{ij})$ is the sum of the constraints imposed by all joints in the manipulator.

The value of λ_i can be identified from the kinematic structure of the links and geometry of each branch. For example, if the ith branch in a planar manipulator has prismatic joints only (two or more joints), then λ_i=2 because, in this case, the branch would allow the mobile platform to have only two translations in the plane and would not allow for any rotation. If, on the other hand, the ith branch in the planar manipulator has revolute joints, then λ_i=3 because, in this case, the branch would allow the mobile platform to have two translations on the plane of motion and a rotation about an axis perpendicular to the plane. Moreover, if the ith branch has revolute

or spherical joints that allow for the mobile platform to move out of the plane, then λ_i=6. Moreover, because the mobile platform is moved and constrained by the branches, the DOF of the motion space of the mobile platform, λ_p, has to be equal to the DOF of the smallest branch motion space, provided that this motion space is not outside the motion space of the other branches. Rearranging equation (2) results in

$$M = \sum_{i=1}^{L}(\lambda_i l_i) + \lambda_p - \sum_{i=1}^{L}\lambda_i n_i + \sum_{i=1}^{L} f_i \qquad : \; f_i = \sum_{j=1}^{n_i} f_{ij} \tag{3}$$

Since $n_i = l_i + 1$ then

$$M = \sum_{i=1}^{L}(\lambda_i l_i) + \lambda_p - \sum_{i=1}^{L}(\lambda_i l_i) - \sum_{i=1}^{L}\lambda_i + \sum_{i=1}^{L} f_i \tag{4}$$

Equation (4) could be written as:

$$M = \sum_{i=1}^{L}(f_i - \lambda_i) + \lambda_p \tag{5}$$

Using equation (5), one could find the correct mobility of parallel manipulators where the DOF of the branch motion spaces are not the same, such as the manipulator shown in Figure 2. If the DOF of the branch motion spaces are the same, equation (5) could be written as:

$$M = \sum_{i=1}^{L}(f_i) - \lambda L + \lambda \tag{6}$$

Equation (6) is the same as presented by Malik and Kerr (1992).

2.1.2 Effect of Joint Jam on Manipulator Mobility

Jamming of a specific joint could change λ_i and λ_p depending on the type of the jammed joint. For example, if the *i*th branch has one revolute and two prismatic joints, then if a revolute joint is jammed, the value of λ_i will be changed from 3 to 2. However, in cases where λ_i and λ_p do not

change due to joint jam, one could easily notice, from equation (5), that the jam of a single-DOF *j*th joint in *i*th branch (i.e., when f_{ij} becomes 0) decreases the mobility by 1.

2.1.3 Effect of Actuator Force Loss on Manipulator Mobility

The loss of the actuator force does not change the mobility of the manipulator because all the terms in equation (5) remain unchanged. However, if the actuator force loss is due to active branch loss, then the mobility changes. From equation (5), if λ_p does not change after branch loss, then one could easily notice that losing the *i*th branch changes the mobility by $(f_i - \lambda_i)$. Therefore, the mobility of the manipulator decreases if $(f_i - \lambda_i) > 0$ and, on the other hand, the mobility of the manipulator increases if $(f_i - \lambda_i) < 0$. The mobility of the manipulator remains unchanged if $(f_i - \lambda_i) = 0$.

2.2 Effect of Active Joint Failure on Manipulator Velocity

2.2.1 Theoretical Background

The theoretical background presented in this sub-section is based on the work of Kumar and Gardner (1990).

For parallel manipulators consisting of a number of serial branches, the velocity equation for the *i*th serial branch is expressed in the following equation:

$$ {}^{i}\dot{\mathbf{x}} = {}^{i}J\ {}^{i}\dot{\mathbf{q}} \quad : \ {}^{i}\dot{\mathbf{x}} \in R^{m},\ {}^{i}\dot{\mathbf{q}} \in R^{n_i}, \text{and } {}^{i}J \in R^{m \times n_i} \ (\text{for } i = 1,2,...L) \tag{7} $$

where ${}^{i}\dot{\mathbf{x}}$ is the vector composed of the components of the linear and/or angular velocity of the end-effector; ${}^{i}\dot{\mathbf{q}}$ is the vector composed of velocities of the joints of the *i*th serial branch; *m* is the dimension of the end-effector motion space, which is assumed to be equal to the dimension of the task space; n_i is the number of the joints of the *i*th branch and ${}^{i}J$ is the Jacobian matrix that maps ${}^{i}\dot{\mathbf{q}}$ to ${}^{i}\dot{\mathbf{x}}$.

In this study, it will be assumed that $m = \lambda =$ (DOF of the task), which is true for 3−DOF planar and 6−DOF spatial manipulators. Therefore, $m=n_i$ (for i=1,.., L) and if the manipulator is in non-singular configuration (^iJ is of full rank), then the velocity of the joints of the ith branch can be calculated from equation (8):

$$^i\dot{\mathbf{q}} = {}^iJ^{-1}\ \dot{\mathbf{x}} \quad : \dot{\mathbf{x}} = {}^i\dot{\mathbf{x}} \qquad (i = 1,2,...,L) \tag{8}$$

where $\dot{\mathbf{x}}$ is the vector composed of the components of the linear and/or angular velocity of the end-effector.

Equation (8) can be written for all the branches in the following compact form:

$$\begin{bmatrix} {}^1\dot{\mathbf{q}} \\ \vdots \\ {}^i\dot{\mathbf{q}} \\ \vdots \\ {}^L\dot{\mathbf{q}} \end{bmatrix} = \begin{bmatrix} {}^1J^{-1} \\ \vdots \\ {}^iJ^{-1} \\ \vdots \\ {}^LJ^{-1} \end{bmatrix} \dot{\mathbf{x}} \tag{9}$$

Reordering the velocities of the joints and their corresponding rows in equation (9), and regrouping the velocities of the active joints and passive joints, separately, results in

$$\dot{\mathbf{q}}_a = J_a^{-1}\ \dot{\mathbf{x}} \qquad : \dot{\mathbf{x}} \in R^m, \dot{\mathbf{q}}_a \in R^{n_a}, \text{and } J_a^{-1} \in R^{n_a \times m} \tag{10}$$

$$\dot{\mathbf{q}}_p = J_p^{-1}\ \dot{\mathbf{x}} \qquad : \dot{\mathbf{x}} \in R^m, \dot{\mathbf{q}}_p \in R^{n_p}, \text{and } J_p^{-1} \in R^{n_p \times m} \tag{11}$$

where $\dot{\mathbf{q}}_a$ and $\dot{\mathbf{q}}_p$ are the vectors composed of velocities of the active and passive joints in the manipulator, respectively; n_a and n_p are the number of active and passive joints in the manipulator, respectively; J_a^{-1} is the inverse Jacobian matrix that maps $\dot{\mathbf{x}}$ to $\dot{\mathbf{q}}_a$ and J_p^{-1} is the inverse Jacobian matrix that maps $\dot{\mathbf{x}}$ to $\dot{\mathbf{q}}_p$.

If m=n_a and the manipulator is in non-singular configuration (J_a^{-1} is of full rank), then the end-effector velocity can be determined from the following equation:

$$\dot{\mathbf{x}} = J_a \, \dot{\mathbf{q}}_a \quad : \dot{\mathbf{x}} \in R^m, \dot{\mathbf{q}}_a \in R^{n_a}, \text{and } J_a \in R^{m \times n_a} \tag{12}$$

In equation (12), there is a unique solution of $\dot{\mathbf{x}} \in R^m$ for every $\dot{\mathbf{q}}_a \in R^{n_a}$. In other words, the end-effector can have any velocity in the task space by controlling the velocities of the active joints. Substituting equation (12) in (11), the relationship between the velocities of the active joints and the velocities of the passive joints could be expressed in the following equation:

$$\dot{\mathbf{q}}_p = G_a^p \, \dot{\mathbf{q}}_a \quad : \quad G_a^p = J_p^{-1} J_a \quad (G_a^p \in R^{n_p \times n_a}) \tag{13}$$

2.2.2 Effect of Joint Jam on Manipulator Velocity

When a single−DOF active joint jams in any branch, equation (12) becomes:

$$\dot{\mathbf{x}} = J_a \, \dot{\mathbf{q}}_a \quad : \dot{\mathbf{x}} \in csp(J_a), \dot{\mathbf{q}}_a \in R^{n_a - 1}, \text{ and } J_a \in R^{m \times (n_a - 1)} \tag{14}$$

where $csp(J_a)$ is the column space of the matrix J_a.

In this sub-section, the Jacobian matrix J_a and the velocity vector $\dot{\mathbf{q}}_a$ will denote the reduced Jacobian matrix and velocity vector, respectively, after active joint jam. In equation (14), the column of the Jacobian matrix corresponding to the jammed active joint is eliminated, resulting in reduction of the rank of J_a by 1. Thus, after failure, the dimension of the column space, n_a−1, becomes smaller than the dimension of the desired task space, m. Equation (14) is consistent (has a solution of $\dot{\mathbf{q}}_a \in R^{n_a - 1}$) only for $\dot{\mathbf{x}} \in csp(J_a)$, and there is no solution of $\dot{\mathbf{q}}_a \in R^{n_a - 1}$ if $\dot{\mathbf{x}} \notin csp(J_a)$. In other words, when an active joint jams in a non-redundant parallel manipulator, the dimension of the space, in which the end-effector could move, is reduced by 1, and, hence, the manipulator loses the ability to move the end-effector in a subspace in R^m that does not belong to $csp(J_a)$. To determine how the end-effector velocity, $\dot{\mathbf{x}}$, lies in R^m relative to $csp(J_a)$, $\dot{\mathbf{x}}$ could be divided into the two orthogonal components shown in equation (15).

$$\dot{\mathbf{x}} = proj_{csp(J_a)}(\dot{\mathbf{x}}) \; + \; proj_{csp(J_a)^{\perp}}(\dot{\mathbf{x}}) \tag{15}$$

where $csp(J_a)^{\perp}$ is the orthogonal complement of $csp(J_a)$; $csp(J_a)^{\perp}$ is a subspace that implies a set of all the vectors in R^m that are orthogonal to the vectors in $csp(J_a)$; the $proj_{csp(J_a)}(\dot{\mathbf{x}})$ and $proj_{csp(J_a)^{\perp}}(\dot{\mathbf{x}})$ are the projections of $\dot{\mathbf{x}}$ onto $csp(J_a)$ and $csp(J_a)^{\perp}$, respectively, which can be found from equations (16) and (17), respectively.

$$proj_{csp(J_a)}(\dot{\mathbf{x}}) = B(J_a)\ (B(J_a))^T\ \dot{\mathbf{x}} \tag{16}$$

where $B(J_a)$ is a matrix whose column vectors form an orthonormal basis that spans $csp(J_a)$.

$$proj_{csp(J_a)^{\perp}}(\dot{\mathbf{x}}) = \dot{\mathbf{x}} - proj_{csp(J_a)}(\dot{\mathbf{x}}) \tag{17}$$

A basis of J_a is the set of all linearly independent column vectors of J_a. An orthonormal basis could be constructed from any basis by applying the Gram-Schmidt procedure, Norman (1995). $B(J_a)$ could, alternatively, be determined from the Singular Value Decomposition (SVD) of J_a, Maciejewski (1990).

An alternate method to find $proj_{csp(J_a)^{\perp}}(\dot{\mathbf{x}})$ is by projecting $\dot{\mathbf{x}}$ onto $csp(J_a)^{\perp}$ as presented in the following procedure:

If $\mathbf{u}$ is a vector in $csp(J_a)^{\perp}$ and the set $\{\mathbf{c}_1(J_a),\ \mathbf{c}_2(J_a),\ \cdots\ ,\mathbf{c}_{n_a-1}(J_a)\}$ contain the column vectors of the matrix J_a, then $\mathbf{u}$ is orthogonal to all the column vectors of J_a. This is represented by the scalar product shown in equation (18).

$$\begin{bmatrix} (\mathbf{c}_1(J_a))^T \\ \vdots \\ (\mathbf{c}_{n_a-1}(J_a))^T \end{bmatrix} \mathbf{u} = 0 \qquad : \begin{bmatrix} (\mathbf{c}_1(J_a))^T \\ \vdots \\ (\mathbf{c}_{n_a-1}(J_a))^T \end{bmatrix} = J_a^T \tag{18}$$

One could notice from equation (18) that the solution of **u** lies in the null space of J_a^T. Therefore, all vectors belonging to $csp(J_a)^{\perp}$ lie in the null space of J_a^T. The null space of J_a^T will be represented by $nsp(J_a^T)$. It is concluded that $csp(J_a)^{\perp} = nsp(J_a^T)$ and $csp(J_a) = nsp(J_a^T)^{\perp}$.

Since $nsp(J_a^T) = csp(N(J_a^T))$, then $csp(J_a)^{\perp} = csp(N(J_a^T))$, where $N\left(J_a^T\right)$ is a matrix whose columns form an orthonormal basis for the null space of J_a^T. $N(J_a^T)$ could be determined from the SVD of J_a^T.

Therefore, $proj_{csp(J_a)^{\perp}}(\dot{\mathbf{x}})$ can be found by projecting $\dot{\mathbf{x}}$ onto the $csp(N(J_a^T))$ as follows:

$$proj_{csp(J_a)^{\perp}}(\dot{\mathbf{x}}) = N\left(J_a^T\right)\left(N\left(J_a^T\right)\right)^T \dot{\mathbf{x}} \tag{19}$$

If $\left(N\left(J_a^T\right)\right)^T \dot{\mathbf{x}} = 0$ (i.e., $proj_{csp(J_a)^{\perp}}(\dot{\mathbf{x}}) = 0$), then $\dot{\mathbf{x}} \in csp(J_a)$. If, however, $\left(N\left(J_a^T\right)\right)^T \dot{\mathbf{x}} \neq 0$ then $\dot{\mathbf{x}} \notin csp(J_a)$ and, hence, the end-effector velocity is not realizable by the manipulator after joint jam. It should be noted that the number of rows and number of columns of $N\left(J_a^T\right)$ equal the number of rows of J_a^T and the dimension of the null space of J_a^T, respectively. The dimension of the null space of J_a^T can be found from equation (20), Nakamura (1991).

$$\dim\, nsp(J_a^T) = (\#\text{of columns of } J_a^T) - \dim\, csp(J_a^T) \tag{20}$$

In case of jam in one of the active single−DOF joints, then $\dim\, nsp(J_a^T) = 1$.

2.2.3 Effect of Actuator Force Loss on Manipulator Velocity

When a parallel manipulator loses the force of one of its actuators, equation (10) becomes

$$\dot{\mathbf{q}}_a = J_a^{-1}\dot{\mathbf{x}} \qquad : \dot{\mathbf{x}} \in R^m, \dot{\mathbf{q}}_a \in R^{n_a-1} \text{ and } J_a^{-1} \in R^{(n_a-1)\times m} \tag{21}$$

In this sub-section, the inverse Jacobian matrix J_a^{-1} and the velocity vector $\dot{\mathbf{q}}_a$ will denote the reduced inverse Jacobian matrix and velocity vector, respectively, after actuator force loss. The

inverse Jacobian matrix, J_a^{-1}, in equation (21) loses the row corresponding to the active joint whose force was lost. Because the number of independent rows of J_a^{-1} in equation (21) becomes smaller than the number of columns after failure, J_a^{-1} has a null space, $nsp(J_a^{-1})$, in which $\dot{\mathbf{q}}_a = 0$ for all $\dot{\mathbf{x}} \in nsp(J_a^{-1})$, indicating that the end-effector could have an unconstrained motion of $\dot{\mathbf{x}} \in nsp(J_a^{-1})$ even if all remaining active joints are locked. To determine how the end-effector velocity, $\dot{\mathbf{x}}$, lies in R^m relative to $nsp(J_a^{-1})$, $\dot{\mathbf{x}}$ could be divided into the two orthogonal components shown in equation (22):

$$\dot{\mathbf{x}} = proj_{nsp(J_a^{-1})}(\dot{\mathbf{x}}) + proj_{nsp(J_a^{-1})^{\perp}}(\dot{\mathbf{x}}) \tag{22}$$

where $nsp(J_a^{-1})^{\perp}$ is the orthogonal complement of $nsp(J_a^{-1})$; $proj_{nsp(J_a^{-1})}(\dot{\mathbf{x}})$ and $proj_{nsp(J_a^{-1})^{\perp}}(\dot{\mathbf{x}})$ are the projections of $\dot{\mathbf{x}}$ onto $nsp(J_a^{-1})$ and $nsp(J_a^{-1})^{\perp}$, respectively; and can be represented as $proj_{nsp(J_a^{-1})}(\dot{\mathbf{x}}) = N\left(J_a^{-1}\right)\left(N\left(J_a^{-1}\right)\right)^T \dot{\mathbf{x}}$ and $proj_{nsp(J_a^{-1})^{\perp}}(\dot{\mathbf{x}}) = \dot{\mathbf{x}} - proj_{nsp(J_a^{-1})}(\dot{\mathbf{x}})$, respectively. Similarly, since $nsp(J_a^{-1})^{\perp} = csp(J_a^{-T})$, then any basis for $csp(J_a^{-T})$ is a basis for $nsp(J_a^{-1})^{\perp}$ and $proj_{nsp(J_a^{-1})^{\perp}}(\dot{\mathbf{x}})$ could, alternatively, be found as $proj_{nsp(J_a^{-1})^{\perp}}(\dot{\mathbf{x}}) = B(J_a^{-T})\ (B(J_a^{-T}))^T \dot{\mathbf{x}}$.

If $(B(J_a^{-T}))^T \dot{\mathbf{x}} = 0$ (i.e., $proj_{nsp(J_a^{-1})^{\perp}}(\dot{\mathbf{x}}) = 0$), then $\dot{\mathbf{x}} \in nsp(J_a^{-1})$, and therefore the end-effector velocity is unconstrained and cannot be controlled by remaining actuators. Meanwhile, if $\left(N\left(J_a^{-1}\right)\right)^T \dot{\mathbf{x}} = 0$ (i.e., $proj_{nsp(J_a^{-1})}(\dot{\mathbf{x}}) = 0$), then $\dot{\mathbf{x}} \in nsp(J_a^{-1})^{\perp}$, and therefore, the end-effector velocity is controllable by the remaining actuator forces. If, however, $proj_{nsp(J_a^{-1})}(\dot{\mathbf{x}}) \neq 0$ and $proj_{nsp(J_a^{-1})^{\perp}}(\dot{\mathbf{x}}) \neq 0$, then $\dot{\mathbf{x}}$ belongs to the union of both of $nsp(J_a^{-1})$ and $nsp(J_a^{-1})^{\perp}$, which

indicates that part of the end-effector velocity is controllable and the other is an unconstrained motion.

2.3 Effect of Active Joint Failure on Manipulator Force

2.3.1 Theoretical Background

The static force equation of the manipulator could be derived based on the principle of virtual work. The derivation neglects the effect of inertial forces, gravity and friction. The virtual work done by actuator forces and end-effector force can be written as:

$$\delta w = \boldsymbol{\tau}_a^T \delta \mathbf{q}_a - \mathbf{F}^T \delta \mathbf{x} \quad : \ \boldsymbol{\tau}_a, \delta \mathbf{q}_a \in R^{n_a}, \text{ and } \mathbf{F}, \delta \mathbf{x} \in R^m \tag{23}$$

where $\boldsymbol{\tau}_a$ is the vector of forces of the active joints in the manipulator (forces for prismatic joints and torques for revolute joints); $\mathbf{F}$ is the vector composed of the components of the linear force and/or moment exerted by the end-effector; $\delta \mathbf{q}_a$ is the vector of virtual displacements of the active joints; $\delta \mathbf{x}$ is the virtual displacement vector of the end-effector. Substituting $\delta w = 0$ and $\delta \mathbf{x} = J_a \, \delta \mathbf{q}_a$ in equation (23), then

$$\boldsymbol{\tau}_a = J_a^T \mathbf{F} \quad : \boldsymbol{\tau}_a \in R^{n_a}, \ \mathbf{F} \in R^m, \text{and } J_a^T \in R^{n_a \times m} \tag{24}$$

If m=n_a and the manipulator is in non-singular configuration (J_a is of full rank), then the forces of the active joints can be determined from equation (25).

$$\mathbf{F} = J_a^{-T} \boldsymbol{\tau}_a \quad : \mathbf{F} \in R^m, \boldsymbol{\tau}_a \in R^{n_a} \text{ and } J_a^{-T} \in R^{m \times n_a} \tag{25}$$

2.3.2 Effect of Joint Jam on Manipulator Force

When a single-DOF acive joint jams in the parallel manipulator, equation (24) becomes:

$$\boldsymbol{\tau}_a = J_a^T \mathbf{F} \quad : \boldsymbol{\tau}_a \in R^{n_a - 1}, \ \mathbf{F} \in R^m, \text{and } J_a^T \in R^{(n_a - 1) \times m} \tag{26}$$

In this sub-section, the vector $\boldsymbol{\tau}_a$ will denote the reduced force vector after active joint jam. After active joint jam, the number of rows of the matrix J_a^T becomes smaller than the number of

columns and, therefore, J_a^T, has a null space, $nsp(J_a^T)$, in which $\boldsymbol{\tau}_a = 0$ for all $\mathbf{F} \in nsp(J_a^T)$. Having $\boldsymbol{\tau}_a = 0$ indicates that the external load on the end-effector is resisted by the structure of the manipulator, not by the actuator forces. Any external force in the task space, $\mathbf{F} \in R^m$, applied on the end-effector can be divided into two orthogonal components:

$$\mathbf{F} = proj_{nsp(J_a^T)}(\mathbf{F}) \; + \; proj_{nsp(J_a^T)^{\perp}}(\mathbf{F}) \tag{27}$$

where $proj_{nsp(J_a^T)}(\mathbf{F}) = N\left(J_a^T\right)\left(N\left(J_a^T\right)\right)^T \mathbf{F}$ and $proj_{nsp(J_a^T)^{\perp}}(\mathbf{F}) = B(J_a)\ (B(J_a))^T\ \mathbf{F}$.

If $(B(J_a))^T\ \mathbf{F} = 0$, then $\mathbf{F} \in nsp(J_a^T)$, and therefore, the external force exerted on the end-effector is resisted by the structure of the manipulator. Meanwhile, if $\left(N\left(J_a^T\right)\right)^T\ \mathbf{F} = 0$, then $\mathbf{F} \in nsp(J_a^T)^{\perp}$, and therefore, the external end-effector force on the end-effector is resisted by actuator forces. If, however, $(B(J_a))^T\ \mathbf{F} \neq 0$ and $\left(N\left(J_a^T\right)\right)^T\ \mathbf{F} \neq 0$, then $\mathbf{F}$ belongs to the union of $nsp(J_a^T)$ and $nsp(J_a^T)^{\perp}$, and therefore, part of the external force applied on the end-effector is resisted by the actuator forces and the other part is resisted by the manipulator structure.

2.3.3 Effect of Actuator Force Loss on Manipulator Force

As a result of actuator force loss, equation (25) becomes:

$$\mathbf{F} = J_a^{-T}\,\boldsymbol{\tau}_a \quad : \mathbf{F} \in R^m;\ \boldsymbol{\tau}_a \in R^{n_a-1};\ \text{and}\ J_a^{-T} \in R^{m\times(n_a-1)} \tag{28}$$

The number of columns of the matrix, J_a^{-T}, after actuator force loss, becomes smaller than the number of rows and, therefore, the dimension of the column space, n_a–1, becomes smaller than the dimension of the desired task space, m. In this case, there is no solution of $\boldsymbol{\tau}_a \in R^{n_a-1}$ for any vector $\mathbf{F} \notin csp(J_a^{-T})$. Force applied on the end-effector, $\mathbf{F} \in R^m$, could be divided into two orthogonal components:

$$\mathbf{F} = proj_{csp(J_a^{-T})}(\mathbf{F}) \; + \; proj_{csp(J_a^{-T})^{\perp}}(\mathbf{F}) \tag{29}$$

where $proj_{csp(J_a^{-T})}(\mathbf{F}) = B(J_a^{-T})\ (B(J_a^{-T}))^T\ \mathbf{F}$ and $proj_{csp(J_a^{-T})^{\perp}}(\mathbf{F}) = N\left(J_a^{-1}\right)\left(N\left(J_a^{-1}\right)\right)^T\ \mathbf{F}$.

If $\left(N\left(J_a^{-1}\right)\right)^T \mathbf{F} = 0$, then $\mathbf{F} \in csp(J_a^{-T})$ and therefore, the external end-effector force is completely resisted by the actuator forces. If, however, $(B(J_a^{-T}))^T\ \mathbf{F} = 0$, then $\mathbf{F} \in csp(J_a^{-T})^{\perp}$ and therefore, the external force on the end-effector cannot be resisted by the remaining actuator forces, in which case, resulting in unconstrained motion. If, however, $\left(N\left(J_a^{-1}\right)\right)^T \mathbf{F} \neq 0$ and $(B(J_a^{-T}))^T\ \mathbf{F} \neq 0$, then only part of the external force is resisted by the actuator forces.

3. Example

The determination of the post-failure velocity and static force capability is illustrated on the 3-3 Stewart-Gough platform whose schematic diagram is shown in Figure 3. The diagram shows six extensible branches connecting a mobile platform to a fixed base by two sets of concentric spherical joints located at points A_i and B_i, which form two equilateral triangles in the fixed base link and moving platform, respectively. The points A_i and B_i, are located at distances a=0.3m and b=0.2m, respectively, from the triangle centers, O and P, respectively. An *x*-*y*-*z* coordinate frame is attached to the fixed base at its center O, where the *x* and *y* axes lie on the fixed base, with *x*-axis pointing in a direction opposite to OA_3 and *z* pointing out of the plane of the fixed base. The vector $\mathbf{d}_i$ points from A_i to B_i and is expressed in the *x*-*y*-*z* coordinate frame.

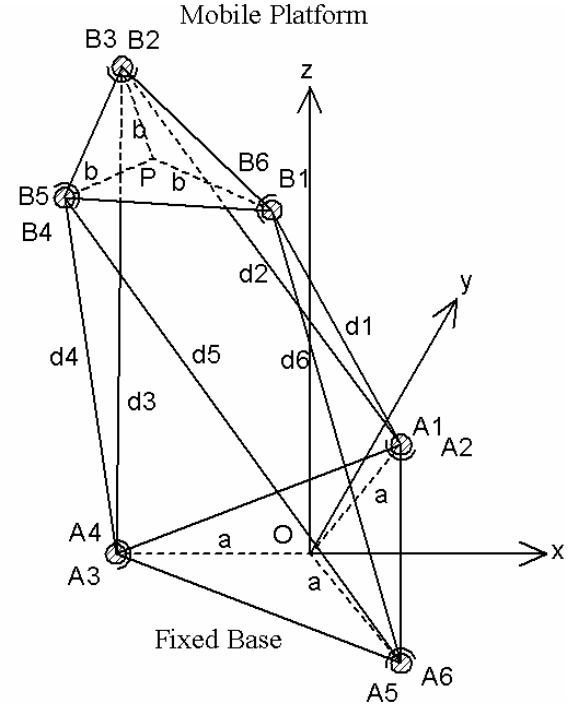

Figure 3: A schematic diagram of the spatial 6-DOF 3-3 Stewart-Gough platform.

The velocity equation (10) for the 3-3 Stewart-Gough platform can be written as, Tsai (1999),

$$\begin{bmatrix} \dot{d}_1 \\ \vdots \\ \dot{d}_6 \end{bmatrix} = J_a^{-1} \begin{bmatrix} \mathbf{v}_p \\ \boldsymbol{\omega} \end{bmatrix} \qquad : J_a^{-1} = \begin{bmatrix} \mathbf{s}_1^T & (\mathbf{b}_1 \times \mathbf{s}_1)^T \\ \mathbf{s}_2^T & (\mathbf{b}_2 \times \mathbf{s}_2)^T \\ \vdots & \vdots \\ \mathbf{s}_6^T & (\mathbf{b}_6 \times \mathbf{s}_6)^T \end{bmatrix}; \quad \mathbf{v}_p = \begin{bmatrix} v_{px} \\ v_{py} \\ v_{pz} \end{bmatrix}; \; \boldsymbol{\omega} = \begin{bmatrix} \omega_x \\ \omega_y \\ \omega_z \end{bmatrix} \tag{30}$$

where $\mathbf{v}_p$ is the velocity vector of point P; $\boldsymbol{\omega}$ is the angular velocity vector of the mobile platform; $\dot{d}_i$ is the rate of the prismatic active joint in *i*th branch; $\mathbf{s}_i$ is a unit vector along the direction of the *i*th branch; $\mathbf{b}_i$ is the vector extended from point P to point B_i. The rotations of the moving link is expressed by vector $\boldsymbol{\theta} = [\theta_x, \theta_y, \theta_z]^T$ (degrees) while the position of point P with respect to point O is expressed by vector $\mathbf{p} = [p_x, p_y, p_z]^T$ (meter). All vectors are expressed in the *x*-*y*-*z* coordinates. To predict the velocity and force of the manipulator after the active joint in branch 2 is jammed, the second column of matrix J_a, which is obtained by taking the inverse

of J_a^{-1} in equation (30), is eliminated and $N\left(J_a^T\right)$ is determined. On the other hand, to predict the velocity and force of the manipulator after actuator force loss in branch 2, the second row of matrix J_a^{-1} is eliminated and $N\left(J_a^{-1}\right)$ is determined. In accordance with the analysis of Sections 2.2 and 2.3 the equation of the velocities and forces of the example manipulator of Figure 3 after failure are listed in Tables 1 and 2.

Table 1: Velocity and force criteria after active joint jam in branch 2.

Configuration: $\mathbf{p}=[p_x,p_y,p_z]^T$ (meter), $\boldsymbol{\theta}=[\theta_x,\theta_y,\theta_z]^T$ (deg)	**Velocity Criteria** $\left(N\left(J_a^T\right)\right)^T\ \dot{\mathbf{x}}=0$	**Force Criteria** $\left(N\left(J_a^T\right)\right)^T\ \mathbf{F}=0$
$\mathbf{p}=[0,0,.7]^T$, $\boldsymbol{\theta}=[0,0,0]^T$	$(.328)v_x+(.114)v_y-(.917)v_z$ $-(.159)w_x-(.092)w_y-(.068)w_z=0$	$(.328)F_x+(.114)F_y-(.917)F_z$ $-(.159)M_x-(.092)M_y-(.068)M_z=0$
$\mathbf{p}=[.2,-.3,.7]^T$, $\boldsymbol{\theta}=[0,0,0]^T$	$-(.061)v_x-(.475)v_y+(.859)v_z$ $+(.149)w_x+(.086)w_y+(.058)w_z=0$	$-(.061)F_x-(.475)F_y+(.859)F_z$ $+(.149)M_x+(.086)M_y+(.058)M_z=0$
$\mathbf{p}=[0,0,.7]^T$, $\boldsymbol{\theta}=[20,10,30]^T$	$-(.357)v_x-(.189)v_y+(.900)v_z$ $+(.101)w_x+(.115)w_y+(.064)w_z=0$	$-(.357)F_x-(.189)F_y+(.900)F_z$ $+(.101)M_x+(.115)M_y+(.064)M_z=0$
$\mathbf{p}=[.2,-.3,.7]^T$, $\boldsymbol{\theta}=[20,10,30]^T$	$(.116)v_x+(.494)v_y-(.837)v_z$ $-(.119)w_x-(.123)w_y-(.090)w_z=0$	$(.116)F_x+(.494)F_y-(.837)F_z$ $-(.119)M_x-(.123)M_y-(.090)M_z=0$

Table 2: Velocity and force criteria after actuator force loss in branch 2.

Configuration: $\mathbf{p}=[p_x,p_y,p_z]^T$ (meter), $\boldsymbol{\theta}=[\theta_x,\theta_y,\theta_z]^T$ (deg)	**Velocity Criteria** $\left(N\left(J_a^{-1}\right)\right)^T\ \dot{\mathbf{x}}=0$	**Force Criteria** $\left(N\left(J_a^{-1}\right)\right)^T\ \mathbf{F}=0$
$\mathbf{p}=[0,0,.7]^T$, $\boldsymbol{\theta}=[0,0,0]^T$	$-(.263)v_x-(.152)v_y+(.056)v_z$ $+(.542)w_x+(.188)w_y+(.759)w_z=0$	$-(.263)F_x-(.152)F_y+(.056)F_z$ $+(.542)M_x+(.188)M_y+(.759)M_z=0$
$\mathbf{p}=[.2,-.3,.7]^T$, $\boldsymbol{\theta}=[0,0,0]^T$	$-(.234)v_x-(.135)v_y+(.059)v_z$ $+(.674)w_x-(.122)w_y+(.674)w_z=0$	$-(.234)F_x-(.135)F_y+(.059)F_z$ $+(.674)M_x-(.122)M_y+(.674)M_z=0$
$\mathbf{p}=[0,0,.7]^T$, $\boldsymbol{\theta}=[20,10,30]^T$	$-(.255)v_x-(.159)v_y+(.034)v_z$ $+(.228)w_x+(.267)w_y+(.886)w_z=0$	$-(.255)F_x-(.159)F_y+(.034)F_z$ $+(.228)M_x+(.267)M_y+(.886)M_z=0$
$\mathbf{p}=[.2,-.3,.7]^T$, $\boldsymbol{\theta}=[20,10,30]^T$	$(.253)v_x+(.157)v_y-(.043)v_z$ $-(.457)w_x+(.127)w_y-(.827)w_z=0$	$(.253)F_x+(.157)F_y-(.043)F_z$ $-(.457)M_x+(.127)M_y-(.827)M_z=0$

Before failure, the end-effector of 6-DOF 3-3 Stewart-Gough platform can have any velocity, $\dot{\mathbf{x}}$, and apply any force, $\mathbf{F}$, in the 6-dimensional task space. From Tables 1 and 2, it is noticed that after failure of one of the active joints, the velocity and force of the manipulator form two 5-dimensional hyperplanes in R^6. Velocities and forces belonging to the corresponding hyperplanes must satisfy the hyperplane equations. The manipulator cannot have an end-effector velocity or exert any end-effector forces that do not belong to the corresponding 5-dimensional hyperplane. The coefficients of the velocity and force components in Table 1 form the vector that is normal to the 5-dimensional hyperplanes of the reduced velocity and force space after joint jam. In Table 2, the coefficients of the velocity and force components form the vector that is orthogonal to the 5-dimensional hyperplanes of the reduced velocity and force space after actuator force loss. Any force projected on the orthogonal vector is unconstrained and the manipulator will have uncontrollable motion. By applying this analysis, one could simulate the post-failure motion and workspace of the manipulator and determine the capability of the manipulator to exert the desired task force in any configuration during the motion simulation. This information could be obtained analytically before deciding to repair the manipulator or abort the task.

4. Conclusion

The reduced velocity and force capabilities of parallel robots after joint jam and loss of actuator force could be determined by finding the null space vectors of the transpose of the Jacobian matrix and its inverse, respectively. Prediction of the post-failure velocity and force performance of the manipulator is useful for maintenance planning when the manipulator operates in remote, hazardous environments or when failure is critical in the operation. In these circumstances, knowing whether or not the manipulator is still capable of completing the task could be very

critical. The results of the analysis in this study could be used to determine the error between the post-failure actual motion and the desired motion specified by the task. Also, knowledge of the effect of active joint failure on the velocity and force capability of the manipulator will enable designers to incorporate measures to overcome the reduced performance and provide fault tolerance. Currently the effect of having redundant hardware components in providing fault tolerance against active joint failure is being explored.

References

[1] Bergerman, M. and Xu, Y., "Dexterity of Underactuated Manipulators", Int. Conf. of Advanced Robotics, July 1997, pp.719-724.

[2] English, J.D. and Maciejewski, A.A., "Fault Tolerance for Kinematically Redundant Manipulators: Anticipating Free-Swinging Joint Failures", IEEE Transactions on Robotics and Automation, v.14, n.4, 1998, pp.566-575.

[3] Kumar, V. and Gardner, J., "Kinematics of Redundantly Actuated Closed Chains", IEEE Transactions on Robotics and Automation, v.6, n.2, 1990, pp.269-274.

[4] Liu, C.S. and Yu, C.H., "Identification and Classification of Multi-Degree-of-Freedom and Multi-Loop Mechanisms", Trans. ASME, Journal of Mechanical Design, v.117, 1995, pp.104-108.

[5] Maciejewski, A.A., "Fault Tolerant Properties of Kinematically redundant Manipulators", Proc. IEEE International Conference on Robotics and Automation, 1990, pp.638-642.

[6] Malik, A.N. and Kerr, D.R., "New Approach to Type Synthesis of Spatial Robotic Mechanisms", Robotics, Spatial Mechanisms, and Mechanical Systems ASME, Design Engineering Division, v.45, 1992. pp.387-395.

[7] Nakamura, Y., “Advanced Robotics: Redundancy and Optimization”, Addison-Wesley Publishing Company, 1991.

[8] Norman, D., “Introduction to Linear Algebra for Science and Engineering”, Addison-Wesley Publishers, 1995.

[9] Notash, L. and Huang, L., “On the Design of Fault Tolerant Parallel Manipulators”, Mechanism and Machine Theory, v.38, n.1, 2003, pp.85-101.

[10] Roberts, R.G. and Maciejewski, A.A., “A Local Measure of Fault Tolerance for Kinematically Redundant Manipulators”, IEEE Transactions on Robotics and Automation, v.12, n.4,1996, pp.543-552.

[11] Roberts, R.G., “The Dexterity and Singularities of an Underactuated Robot”, Journal of Robotic Systems, v.18, n.4, 2001, pp.159-169.

[12] Ting, Y., Tosunoglu, S. and Freeman, R., “Torque Redistribution and Time Regulation Methods for Actuator Saturation Avoidance of Fault-Tolerant Parallel Robots”, Journal of Robotic Systems, v.12, n.12, 1995, pp.807-820.

[13] Tsai, L.W, “Robot Analysis: The Mechanics of Serial and Parallel Manipulators”, Wiley-Interscience Publication, 1999.

[14] Visinsky, M.L., Cavallaro, J.R. and Walker, J.R., “Robotic Fault Detection and Fault Tolerance: A Survey”, Reliability Engineering and System Safety, v.46, n.2, 1994, pp.139-158.

[15] Zhang, J., “Computerized Analysis and Synthesis Methodologies for Mechanism Design”, Master’s Thesis, Dept. of Mechanical Engineering, Queen’s University, Canada, 2000.